Preparation and Characterization of α-Al_2O_3/Nylon 6 Nanocomposite Masterbatches

Cheng-Ho Chen,[1,2] Hsiang-Yuan Li,[1] Chien-Yuan Chien,[1] Fu-Su Yen,[3] Heng-Yi Chen,[4] Jian-Min Lin[4]

[1]*Department of Chemical and Materials Engineering, Southern Taiwan University, Tainan County, Taiwan*
[2]*Center for Micro/Nano Science and Technology, National Cheng Kung University, Tainan city, Taiwan*
[3]*Department of Resources Engineering, National Cheng Kung University, Tainan city, Taiwan*
[4]*Department of Products, Taiwan Textile Research Institute, Taipei County, Taiwan*

Received 13 October 2007; accepted 20 October 2008
DOI 10.1002/app.29494
Published online 23 January 2009 in Wiley InterScience (www.interscience.wiley.com).

ABSTRACT: In this study, two types of nanoscale α-Al_2O_3 particles were used to prepare α-Al_2O_3/Nylon 6 nanocomposite masterbatches. They were either uncoated or coated with stearic acid. A wide angle X-ray diffractometer was used to examine the crystal structure of virgin pure nylon 6 and α-Al_2O_3/nylon 6 nanocomposite masterbatches. Meanwhile, a differential scanning calorimeter and a thermogravimetric analyzer were used to illustrate the influence of nanoscale α-Al_2O_3 particles on the thermal properties of the α-Al_2O_3/nylon 6 nanocomposite masterbatches. In addition, a field-emission scanning electron microscopy was applied to reveal the dispersion of uncoated or coated α-Al_2O_3 particles in the nylon 6 matrix. Furthermore, an energy dispersive X-ray spectrometer was also conducted to confirm the existence of the aluminum element in the α-Al_2O_3/nylon 6 nanocomposite masterbatches. © 2009 Wiley Periodicals, Inc. J Appl Polym Sci 112: 1063–1069, 2009

Key words: nylon 6; α-Al_2O_3; extrusion; dispersion; nanocomposite

INTRODUCTION

Polymer nanocomposites have been received great attention because these materials often exhibit much better properties than those polymers or polymers filled with micrometer size inorganic filler particles. By adding only 2–5 wt % nanoscale fillers, the enormous enhancement in properties can be observed. Furthermore, the material cost and the weight of finished articles can be obviously reduced for polymer nanocomposites in comparison to those of the conventional polymer microcomposites.[1] Various nanoscale fillers have been studied to improve the mechanical and thermal properties of polymers, such as clay,[2] silica,[3] calcium carbonate ($CaCO_3$),[4–6] and aluminum oxide (Al_2O_3).[7] The improved properties included toughness, stiffness, damping, chemical resistance, heat resistance, thermal conductivity, low coefficient of thermal expansion, and electrical properties.

Nylon 6 (polyamide 6) is an engineering thermoplastic polymer that is well known for its balance of strength, modulus, and chemical resistance. This material is mainly used in the field of fibers and engineering plastics. It also has many potential applications in automobiles, appliances, and other commercial products in which creep resistance, stiffness, and some toughness are demanded in addition to weight and cost savings.[8]

Nylon 6 is a semicrystal polymorphous polymer. It has two major crystal forms, the α-form and the γ-form. The α-form is characterized by a fully extended configuration of the polymer chains that show an antiparallel orientation. Antiparallel chains are situated such that the amide linkage and methylene units lie within the same plane and H-bonds occur between adjacent antiparallel chains to form sheets of H-bonded chains. This structure repeats itself, thereby, creating stacks of H-bonded sheets in a monoclinic crystal. The γ crystal form occurs when H-bonds form between parallel polyamide chains. In this case H-bond formation requires the amide linkages to twist $\sim 60^\circ$ out the plane of these molecular sheets. The chain packing of the γ-form resembles that of a hexagonal structure.[8,9]

For nylon 6 nanocomposites, most papers were focused on the area of clay/nylon 6 nanocomposites. Several studies reported the influence of clay on the crystal structure of nylon 6 as well as the influence

Correspondence to: C.-H. Chen (chchen@mail.stut.edu.tw).
Contract grant sponsor: Taiwan Textile Research Institute.
Contract grant sponsor: Ministry of Economics Affairs, R.O.C.; contract grant number: 93-EC-17-A-08-S1-023.

of the polymer crystal modification on final properties of polyamide based materials.[10–15] Ozisik and coworker[16] studied three effects on the dispersion of clays for clay/nylon 6 nanocomposites. Avella et al.[17] studied the characterization and properties of calcium carbonate/nylon 6 nanocomposites. Meanwhile, Hasan et al.[18] investigated the effect of SiO_2 nanoparticle on the thermal and mechanical properties of nylon 6. Also, Bose et al.[19] studied the effect of coupling agents on the mechanical, thermal, and dielectric properties of mica reinforced nylon 6. Jia and Ling[20] studied the influence of Al_2O_3 reinforcement on the abrasive wear characteristic of Al_2O_3/nylon 1010 composite coatings that the size of Al_2O_3 particles studied was in the range from 40.5 to 161.0 μm. However, according to our literature search, no study has been focused on the area of α-Al_2O_3/nylon 6 nanocomposite masterbatches so far.

Recently, the unwoven fabric prepared by melt blowing process attracts great interests, because of this material can be produced quickly and applied in various fields. To improve the abrasion resistance of unwoven fabric of nylon 6, the nanoscale α-Al_2O_3 particles are quite suitable to be used as the fillers. This is because α-Al_2O_3 has better abrasion resistance and higher thermal property than other inorganic fillers do. Meanwhile, in order not to stop up the holes of spinneret of the melt blowing equipment, not only the nanoscale α-Al_2O_3 particles have to be used but also the dispersion of the nanoscale α-Al_2O_3 particles in the nylon 6 must be as homogenous as possible.

The research goal of this study was to prepare and characterize α-Al_2O_3/nylon 6 nanocomposite masterbatches. A twin-screw extruder was used to prepare the α-Al_2O_3/nylon 6 nanocomposite masterbatches. Normally, it is difficult to disperse inorganic nanoparticles into an organic matrix uniformly by melt blending method without any surface modification. Therefore, two types of α-Al_2O_3 particles were used and compared in this study. One was uncoated α-Al_2O_3 and the other was coated α-Al_2O_3. The uncoated α-Al_2O_3 stands for the α-Al_2O_3 particles without any surface modification and the coated α-Al_2O_3 stands for the α-Al_2O_3 particles with surface modification by stearic acid.

A wide angle X-ray diffractometer (WAXD) was used to examine the crystal structure of virgin pure nylon 6 and α-Al_2O_3/nylon 6 nanocomposites. A differential scanning calorimeter (DSC) and a thermogravimetric analyzer (TGA) were also used to illustrate the influence of nanoscale α-Al_2O_3 particles on the thermal properties of the α-Al_2O_3/nylon 6 nanocomposites. Meanwhile, a field-emission scanning electron microscopy (FESEM) was applied to reveal the dispersion of uncoated or coated α-Al_2O_3 particles in the nylon 6 matrix. In addition, an energy dispersive X-ray spectrometer (EDX) was also conducted to confirm the existence of the aluminum element in the α-Al_2O_3/nylon 6 nanocomposites.

EXPERIMENTAL

Materials

The nanoscale α-Al_2O_3 particles were kindly supplied by the Particulate Materials Research Center (PMRC) at the National Cheng-Kung University, Tainan, Taiwan. The primary crystal phase of α-Al_2O_3 was no less than 99.0 wt %. Its particle size was ranged from 50 to 200 nm and its specific surface area was about 200 m^2/g. The coated α-Al_2O_3 was prepared by suspending nanoscale α-Al_2O_3 particles in an ethanol solution containing 3 wt % stearic acid. After 3-h stirring, the coated α-Al_2O_3 was filtered and dried. The nylon 6 (nylon 6 2NAA) was purchased from the Formosa Chemicals and Fiber Corp., Taiwan. Its relative viscosity was 2.450 ± 0.015 (tested in 96 wt % sulfuric acid).

Preparation of α-Al_2O_3/nylon 6 composites

A twin extruder (Zenix Industrial Co., Ltd., Taiwan, model ZPT-32HT) with a screw diameter of 32 mm, a length-to-diameter ratio (L/D) of 35.5 and 10 temperature zones was used to prepare the 30 wt % α-Al_2O_3/nylon 6 nanocomposite masterbatches by incorporating 30 wt % coated or uncoated α-Al_2O_3 into the nylon 6 matrix. Before the processing, the nylon 6 pellets were dried in a circulating air oven at 80°C for 12 h to remove the moisture. The extrusion process was performed at a screw speed of 60 rpm, temperature of 240°C at Zone 1, temperature of 245°C at Zone 2, temperatures of 250°C at Zones 3–5, temperatures of 255°C at Zones 6–8, and temperatures of 250°C at Zones 9–10.

Wide angle X-ray diffraction examination

The crystal structures of the virgin pure nylon 6 and α-Al_2O_3/nylon 6 nanocomposites were examined by a WAXD (Rigaku Ltd., Japan, model Rigaku multiflex ZD3609*N*). Cu Kα ($\lambda = 0.154$ nm) radiation was adopted at ambient temperature. The scanning rate was set as 2°/min in the range from 10° to 40°.

DSC technique

A differential scanning calorimeter (DSC; Perkin–Elmer, model: DSC 7, USA) was used to examine the thermal and crystallization behaviors of the virgin pure nylon 6 and α-Al_2O_3/nylon 6 nanocomposites under a nitrogen flow. The specimens were excised from extruded strands that were quenched

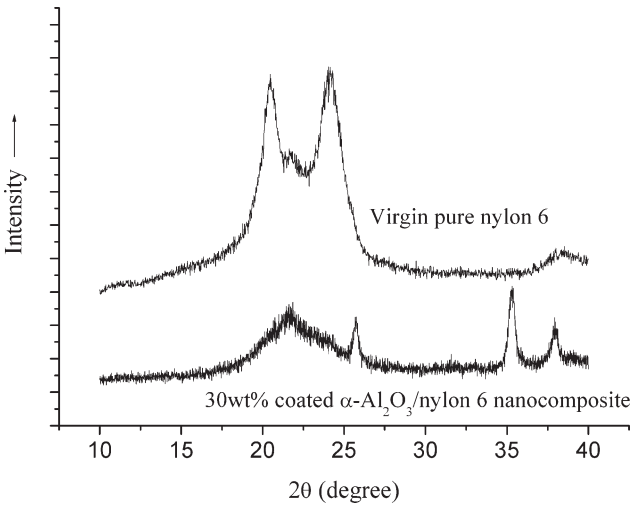

Figure 1 WAXD patterns obtained from the virgin pure nylon 6 and the 30 wt % coated α-Al_2O_3/nylon 6 nanocomposite.

in water, air dried, and pelletized. The resulting specimens were further dried under vacuum for approximate 12 h at 80°C prior to the DSC analysis. The sample was heated and then cooled. This process was repeated twice with various temperature ranges. The first heating–cooling cycle is intended to release the internal stress of the sample. Thus, the sample was heated from 0 to 100°C with a heating rate at 20°C/min and then cooled to 0°C with a cooling rate at 20°C/min. The second cycle is the one used for study. The sample was reheated from 0 to 250°C, held for 1 min to ensure completely melting, and then recooled from 250 to 0°C with a cooling rate at 10°C/min. The heating scan of the second cycle was analyzed for the melting temperature (T_m) and the heat of fusion (ΔH_f). Then, the cooling scan was used to obtain the crystallization temperature (T_c) and heat of crystallization (ΔH_c). The level of crystallinity (χ_c) of the sample was equal to the ratio of $\Delta H_f/\Delta H_f^o$. As the ΔH_f^o values of both crystal forms of nylon 6 are nearly identical (ΔH_f^o of α-form = 241 J/g; ΔH_f^o of γ-form = 239 J/g), the average of the two (i.e., 240 J/g) was adopted for ΔH_f^o.[20]

TGA technique

A thermogravimetric analyzer (TGA; Perkin–Elmer, model: TGA 7, USA) was conducted to analyze the thermal degradation characteristics of the virgin pure nylon 6 and α-Al_2O_3/nylon 6 nanocomposites in the range from 50 to 800°C with a heating rate of 10°C/min under a nitrogen stream. The thermal degradation onset temperature and the thermal degradation weight loss of the samples were recorded and analyzed, respectively.

FESEM Examination

The surface morphologies of the extruded pure nylon 6 and α-Al_2O_3/nylon 6 nanocomposites were examined to reveal the dispersion for the uncoated and coated α-Al_2O_3 particles in the nylon 6 matrix. Each sample was coated with the gold palladium film and examined by a field-emission scanning electron microscopy (FESEM, Jeol Ltd., Japan, model JSM 6700F). The fractured cross sections were prepared by immersing the samples into liquid nitrogen for 45 s. Then, samples were fractured and then further coated with the gold palladium film. To confirm the existence of α-Al_2O_3 particles in the nylon 6

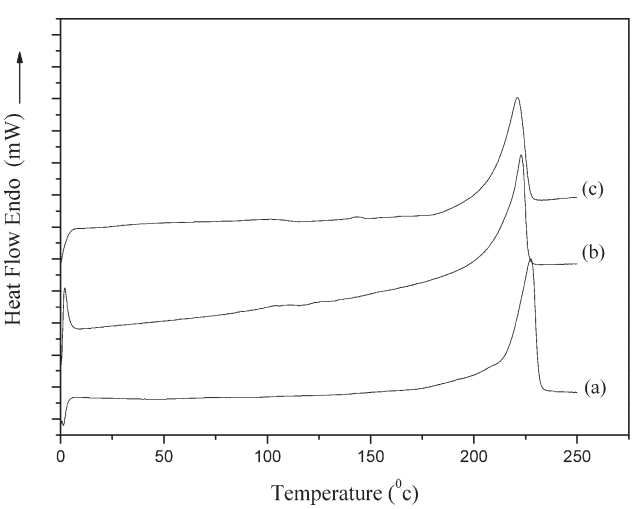

Figure 2 Heating scans of samples (a) virgin pure nylon 6, (b) 30 wt % uncoated α-Al_2O_3/nylon 6 nanocomposite (c) 30 wt % coated α-Al_2O_3/nylon 6 nanocomposite. Scans are shifted for clarity.

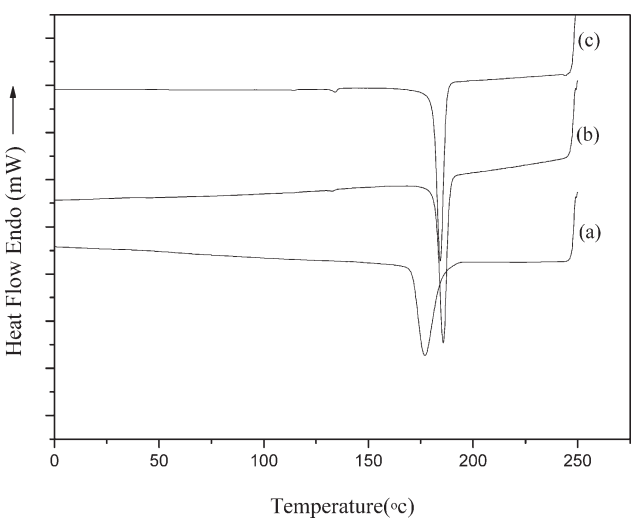

Figure 3 Cooling scans of samples (a) virgin pure nylon 6, (b) 30 wt % uncoated α-Al_2O_3/nylon 6 nanocomposite (c) 30 wt % coated α-Al_2O_3/nylon 6 nanocomposite. Scans are shifted for clarity.

TABLE I
Differential Scanning Calorimetry Data for the Virgin Pure Nylon 6 and its Nanocomposites

Sample	Heating			Cooling	
	T_m(°C)	ΔH_f[a](J/g)	χ_c[b](%)	T_c(°C)	ΔH_c(J/g)
Virgin pure nylon 6	227.5	72.1	30.0	174.5	−71.9
30 wt % uncoated α-Al_2O_3/nylon 6	222.9	96.6	40.2	186.3	−96.6
30 wt % coated α-Al_2O_3/nylon 6	221.0	77.0	32.1	184.3	−71.4

[a] H_f values are based on the amount of pure nylon 6 within the sample.
[b] The level of crystallinity (χ_c) is calculated by the ratio of H_f^o/H_f^o where H_f^o is the average of H_f^o (α-form) and H_f^o (γ-form), i.e., 240 J/g.

matrix, an EDX was also conducted to confirm the existence of aluminum element.

RESULTS AND DISCUSSION

Figure 1 showed the WAXD patterns of the virgin pure nylon 6 (i.e., from as-received pellets) and the 30 wt % coated α-Al_2O_3/nylon 6 nanocomposite, respectively. The WAXD pattern of the virgin pure nylon 6 showed two major diffraction peaks at $2\theta = 20.1°$ and 23.7° that were assigned to the (200) reflection and (002)/(202) reflections of the α-crystalline form of nylon 6, respectively,.[17] Meanwhile, a minor diffraction peak was also observed at $2\theta = 21.3°$, which was the characteristic peak for the γ-crystalline of nylon 6. However, the characteristic peaks of the α-crystalline form of nylon 6 were not observed in the WXRD pattern of the 30 wt % coated α-Al_2O_3/nylon 6 nanocomposite. Only the characteristic peak, $2\theta = 21.3°$, for the γ-crystalline of nylon 6 was observed. This phenomenon was resulted from the rapid cooling of melting nylon 6 from the extruder and this process favored the formation of γ-crystals of nylon 6. Generally speaking, a rapid cooling process induced the nylon 6 to start the crystallization at low temperature and the crystallization rate was limited by polymer chain mobility. Thus, the mobility limitations may be the cause for favoring the formation of γ-crystals of nylon 6.[21] The WAXD patterns of 30 wt % uncoated α-Al_2O_3/nylon 6 and 30 wt % coated α-Al_2O_3/nylon 6 nanocomposites were identical. Therefore, the WAXD pattern of 30 wt % uncoated α-Al_2O_3/nylon 6 nanocomposite was not shown here. From the aforementioned WAXD results, three factors can be considered as the major causes for the formation of the γ-crystals of nylon 6. Firstly, it was due to the rapid cooling of melting α-Al_2O_3/nylon 6 nanocomposite from the extruder favors the formation of γ-crystals of nylon 6. Secondly, adding α-Al_2O_3 particles can decrease the chain mobility and then increase the formation of γ-crystals of the nylon 6. Thirdly, spherical nanoparticles can promote and stabilize the γ-crystals of nylon 6 in the composite.[17] The shape of α-Al_2O_3 particle used in this study was similar to spherical.

Figures 2 and 3 showed the heating and cooling scans of samples taken from the virgin pure nylon 6, 30 wt % uncoated α-Al_2O_3/nylon 6 and 30 wt % coated α-Al_2O_3/nylon 6 nanocomposites, respectively. From these two figures, the heat of fusion (ΔH_f), melting temperature (T_m), level of crystallinity (χ_c), crystallization temperature (T_c) and heat of crystallization (ΔH_c) of the samples were summarized in Table I. Two significant observations were found in Table I. Firstly, the T_m (227.5°C) of the virgin pure nylon 6 was about 5°C higher than those of the 30 wt % α-Al_2O_3/nylon 6 nanocomposites (both for uncoated and coated). This was due to the melting temperature of the α-crystals was higher than that of γ-crystals in nylon 6.[21] Therefore, the γ-crystals of the nylon 6 in the α-Al_2O_3/nylon 6 nanocomposites can be melted under the lower temperature no matter the α-Al_2O_3 particles were surface modified or not. Secondly, the T_c of 30 wt % α-Al_2O_3/nylon 6 nanocomposites (both for uncoated and coated) was about 10–12°C higher than that of the virgin pure nylon 6. Meanwhile, the shapes of crystallization peaks of α-Al_2O_3/nylon 6 nanocomposites were sharper than that of the virgin pure nylon 6 in Figure 3 also. These observations implied that the crystallization rate of nylon 6 in the α-Al_2O_3/nylon 6

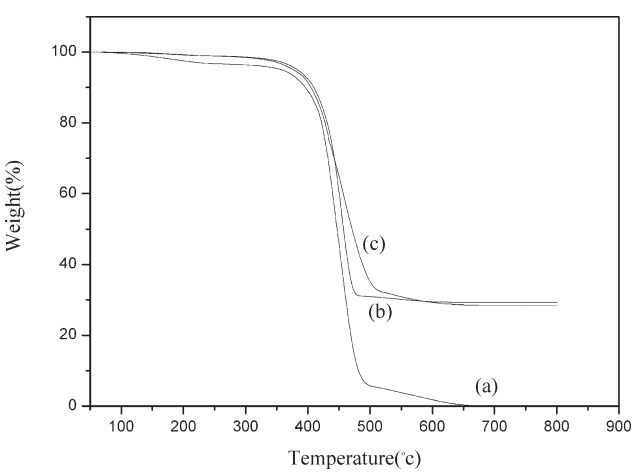

Figure 4 TGA curves of samples (a) virgin pure nylon 6, (b) 30 wt % uncoated α-Al_2O_3/nylon 6 composite (c) 30 wt % coated α-Al_2O_3/nylon 6 nanocomposite.

TABLE II
TGA Data for the Virgin Pure Nylon 6 and its Nanocomposites

Sample	$T_{d,5\%}$(°C)	Residue (%)
Virgin pure nylon 6	357.8	0.0
30 wt % uncoated α-Al_2O_3/nylon 6	383.3	29.6
30 wt % coated α-Al_2O_3/nylon 6	376.5	28.4

$T_{d,5\%}$ is the temperature that the sample remains 95 wt%.

nanocomposites were faster than that of the virgin pure nylon 6. These phenomena were resulted from the nucleation of nylon 6 crystal induced by the nanoscale α-Al_2O_3 particles in the α-Al_2O_3/nylon 6 nanocomposites. Nanoscale α-Al_2O_3 particles can act as an effective nucleating agent in the nylon 6 matrix. Therefore, the level of crystallinity (χ_c) of the nylon 6 in the 30 wt % uncoated α-Al_2O_3/nylon 6 nanocomposite was about 10% higher than that of the virgin pure nylon 6. However, the χ_c of the nylon 6 in the 30 wt % coated α-Al_2O_3/nylon 6 nanocomposite was only 2% higher than that of the virgin pure nylon 6. This might be resulted from the surface modifier of α-Al_2O_3 particles. For nylon 6, the surface modifier was acted as an impurity. Thus, the surface modifier can reduce the χ_c of the nylon 6. Therefore, the χ_c of the nylon 6 in the 30 wt % coated α-Al_2O_3/nylon 6 nanocomposite can not be as high as that of the nylon 6 in the 30 wt % uncoated α-Al_2O_3/nylon 6 nanocomposite.

TGA curves and data of the virgin pure nylon 6 and its nanocomposites were shown on Figure 4 and Table II, respectively. The $T_{d,5\%}$ of the 30 wt % uncoated α-Al_2O_3/nylon 6 nanocomposite was about 383.3°C which was about 25.5°C higher than that of the virgin pure nylon 6. The $T_{d,5\%}$ of the 30 wt % coated α-Al_2O_3/nylon 6 nanocomposite was about 376.5°C and this was about 18.7°C higher than that of the virgin pure nylon 6 also. Results indicated that the $T_{d,5\%}$ of the nylon 6 was significantly increased by the incorporation of 30 wt % nanoscale

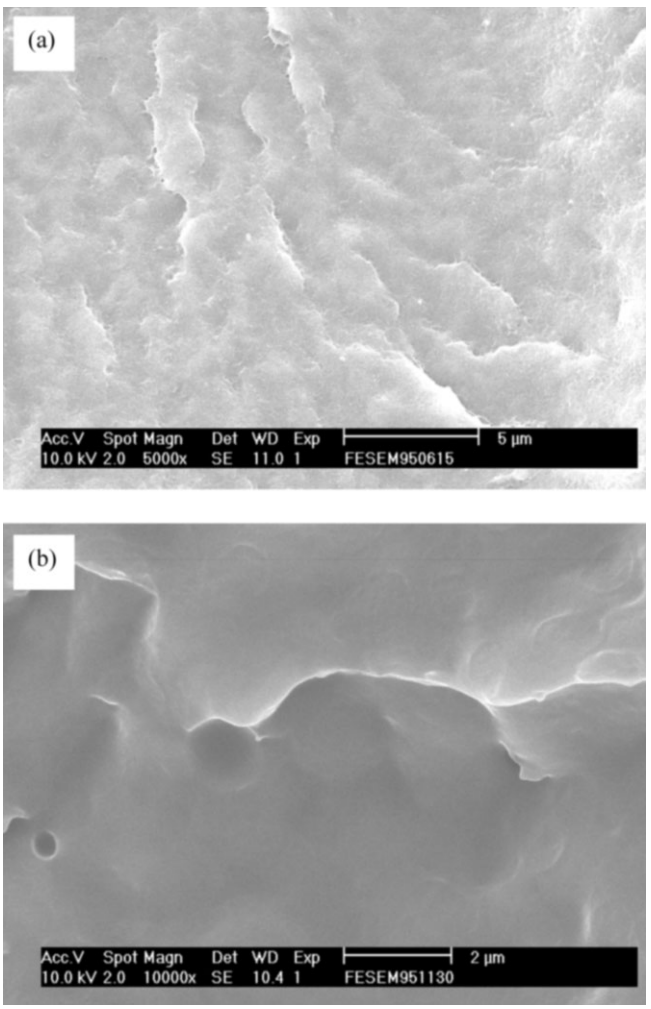

Figure 5 FESEM photographs of the fractured surfaces of the virgin pure nylon 6 (a) ×5,000 (b) ×10,000.

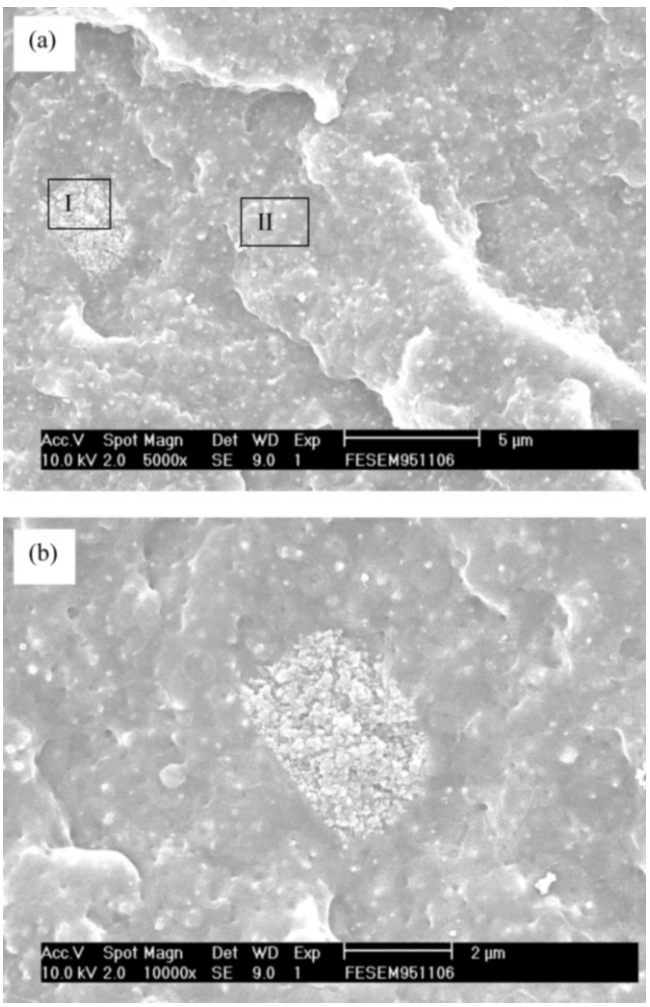

Figure 6 FESEM photographs of the fractured surfaces of 30 wt % uncoated α-Al_2O_3/nylon 6 nanocomposite (a) ×5,000 (b) ×10,000.

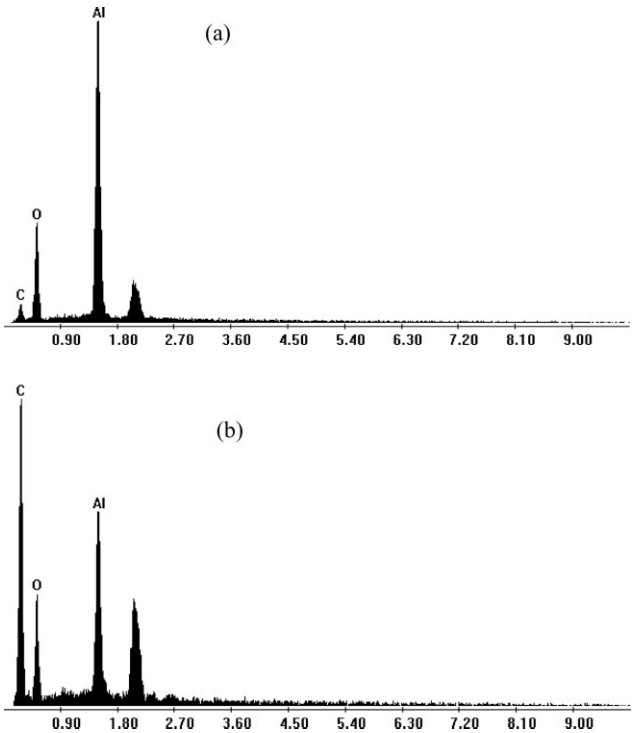

Figure 7 EDX analyses of the fractured surfaces of 30 wt % uncoated α-Al_2O_3/nylon 6 nanocomposite (a) area I shown on Figure 6(a); (b) area II shown on Figure 6(a).

either uncoated or coated α-Al_2O_3 particles into the nylon 6 matrix. The excellent thermal conductivity of α-Al_2O_3 was the major contribution for this observation. However, the $T_{d,5\%}$ of the nylon 6 in the 30 wt % coated α-Al_2O_3/nylon 6 nanocomposite was about 6.8°C lower than that of the 30 wt % uncoated α-Al_2O_3/nylon 6 nanocomposite. This was resulted from the existence of stearic acid (i.e., surface modifier) in the 30 wt % coated α-Al_2O_3/nylon 6 nanocomposite.

Figure 5 showed FESEM photographs (5,000× and 10,000×) of the fractured surface of the virgin pure nylon 6. The fractured surfaces looked smooth in both Figure 5(a,b). Figure 6 showed FESEM photographs (5,000× and 10,000×) of the fractured surface of the 30 wt % uncoated α-Al_2O_3/nylon 6 nanocomposite. By comparison of Figures 5(a) and 6(a), it showed that the cross section of compounded material became rough with adding nanoscale α-Al_2O_3 particles in the nylon 6 matrix. In addition, the nanoscale α-Al_2O_3 particles can be obviously observed in Figure 6(a,b). Figure 6(a,b) also indicated that part of the uncoated α-Al_2O_3 particles were easily aggregated together in the composite. Meanwhile, part of the uncoated α-Al_2O_3 particles can be well dispersed in the nylon 6 matrix. The dispersion of the uncoated α-Al_2O_3 particles were not homogeneous in the nylon 6 matrix.

Figure 7(a,b) displayed the EDX analyses of the fractured surfaces of the 30 wt % uncoated α-Al_2O_3/nylon 6 nanocomposite. These two images were taken from the areas I and II identified in Figure 6(a), respectively. The EDX spectrum of the area I showed very strong signal of aluminum element. The EDX analyses also revealed that the content of aluminum element in area I was much higher than that in area II. This result confirmed the cluster that was formed by the aggregation of many uncoated nanoscale α-Al_2O_3 particles.

Figure 8(a,b) showed FESEM photographs (5,000× and 10,000×) of the fractured surface of the 30 wt % coated α-Al_2O_3/nylon 6 nanocomposite. Comparing Figure 8(a) with Figure 6(a) or comparing Figure 8(b) with Figure 6(b), no significant aggregation of the coated α-Al_2O_3 particles was observed in Figure 8(a) or Figure 8(b). Figure 8(b) showed that most of coated α-Al_2O_3 particles were well dispersed in the TPU matrix. The dispersion improvement was contributed by the surface modification of the nanoscale

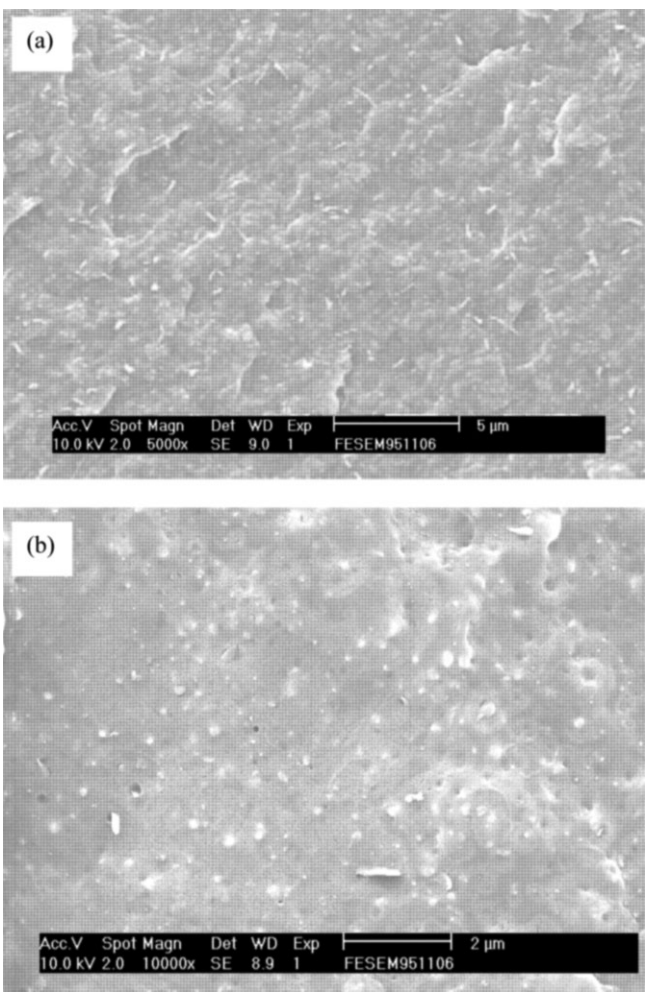

Figure 8 FESEM photographs of the fractured surfaces of 30 wt % coated α-Al_2O_3/nylon 6 nanocomposite (a) ×5,000 (b) ×10,000.

α-Al_2O_3 particles by stearic acid. Thus, the coated α-Al_2O_3 particles were not agglomerated during the extrusion processing.

These observations indicated that stearic acid coated on the surface of the nanoscale α-Al_2O_3 particles can act as a compatibilizer to bridge the boundary between the polymer matrix (nylon 6) and the nanoscale α-Al_2O_3 particles. Please note that stearic acid was a typical fatty acid which contained essentially long hydrocarbon chains. This hydrocarbon chain contained a carboxyl group at one end and a methyl group at the other. Thus, the carboxyl group of stearic acid can form a physical interaction, i.e., hydrogen bond, with the polar surface of α-Al_2O_3. Then, the long hydrocarbon chain, $-CH_3(CH_2)_{16}$, caused the α-Al_2O_3 surface to become hydrophobic. Therefore, the surface modification of α-Al_2O_3 particles by steaeric acid resulted in not only reducing melt viscosity during the melt blending process but also improving the dispersion of coated α-Al_2O_3 in the nylon 6 matrix. From the FESEM results in Figures 6 and 8, it can be concluded that stearic acid was not only a suitable surface modifier for nanoscale α-Al_2O_3 particles, but also a good dispersion promoter between the α-Al_2O_3 particles and nylon 6 matrix.

CONCLUSION

Two types of nanoscale α-Al_2O_3 particles were used for the preparation of α-Al_2O_3/nylon 6 nanocomposite masterbatches. The rapid cooling of the melting α-Al_2O_3/nylon 6 nanocomposite from the extruder enhanced the γ-crystalline form of nylon 6. Meanwhile, adding α-Al_2O_3 particles can decrease chain mobility and then enhance the formation of γ-crystals of nylon 6. In addition, nanoscale α-Al_2O_3 particles can act as an effective nucleating agent in the nylon 6 matrix. Furthermore, the $T_{d,5\%}$ of the nylon 6 was significantly increased by the incorporation of 30 wt % nanoscale uncoated or coated α-Al_2O_3 particles into the nylon 6 matrix. For the uncoated α-Al_2O_3/nylon 6 nanocomposite, FESEM results demonstrated that the uncoated α-Al_2O_3 particles were significantly aggregated to form clusters in the nylon 6 matrix. This phenomenon was resulted from the poor compatibility between the uncoated α-Al_2O_3 and the nylon 6 matrix.

For the coated α-Al_2O_3/nylon 6 nanocomposite, FESEM results demonstrated that many coated α-Al_2O_3 particles were well dispersed within nanoscale in the nylon 6 matrix. In addition, the FESEM results indicated that stearic acid was not only a suitable surface modifier for nanoscale α-Al_2O_3 particles, but also a good dispersion promoter between the α-Al_2O_3 particles and the nylon 6 matrix.

References

1. Wan, C. Y.; Qiao, X. Y.; Zhang, Y.; Zhang, Y. X. Polym Test 2003, 22, 453.
2. Reynaud, E.; Jouen, T.; Gaunthier, C.; Vigier, G.; Varlet, J. Polymer 2001, 42, 8759.
3. Chan, C. M.; Wu, J. S.; Li, J. X.; Cheung, Y. T. Polymer 2002, 43, 2981.
4. Di Lorenzo, M. L.; Errico, M. E.; Avella, M. J Mater Sci 2002, 37, 2351.
5. Avella, M.; Errico, M. E.; Martuscelli, E. Nano Lett 2001, 1, 213.
6. Cao, Y. M.; Sun, J.; Yu, D. H. J Appl Polym Sci 2002, 83, 70.
7. Chen, C. H.; Mao, C. F.; Tsai, M. S.; Yen, F. S.; Lin, J. M.; Tseng, C. H.; Chen, H.-Y. J Appl Polym Sci 2008, 110, 237.
8. Bernado, P.; Alema, C.; Puiggal, J. Macromol Theory Simul 1998, 7, 659.
9. Wu, T. M.; Chen, E. C. Polym Eng Sci 2002, 42, 1141.
10. Martınez-Vazquez, D. G.; Medellın-Rodrıguez, F. J.; Phillips, P. J.; Sanchez-Valdes, S. J Appl Polym Sci 2003, 88, 360.
11. Zhang, G.; Li, Y.; Yan, D. Polym Int 2003, 52, 795.
12. Kyu, T.; Zhou, Z. I.; Zhu, G. C.; Tajuddin, Y.; Qutubuddin, S. J. Polym Sci B: Polym Phys 1996, 34, 1761.
13. Yoon, K. H.; Polk, M. B.; Min, B. G.; Schiraldi, D. A. Polym Int 2004, 53, 2072.
14. Liu, L.; Qi, Z.; Zhu, X. J Appl Polym Sci 1999, 71, 1133.
15. Zhao, Z.; Zheng, W.; Yu, W.; Tian, H.; Li, H. Macromol Rapid Commun 2004, 25, 1340.
16. Yang, K.; Ozisik, R. Polymer 2006, 47, 2849.
17. Avella, M.; Errico, M. E.; Gentile, G. Macromol Symp 2006, 234, 170.
18. Hasan, M. M.; Zhou, Y.; Mahfuz, H.; Jeelani, S. Mater Sci Eng Polym 2006, 45, 181.
19. Bose, S.; Raghu, H.; Mahanwar, P. A. J Appl Polym Sci 2006, 100, 4074.
20. Jia, X.; Ling, X. M. Wear 2005, 258, 1342.
21. Fornes, T. D.; Paul, D. R. Polymer 2003, 44, 3945.